ESCAPE DELIVERABLE D1.1b

SIGNATURE OF CLIMATIC CHANGES IN SURFACE THERMODYNAMIC AND ENERGETIC COUPLINGS

prepared by Françoise Guichard (CNRM-GAME) with contributions from Laurent Kergoat and Eric Mougin (OMP/GET) and Frédéric Hourdin (IPSL/LMD)

1. Introduction

The ESCAPE D1.1a report showed that a particularly large climatic warming occurred over West Africa during the last 60 years (much larger than the global mean, e. g. Roehrig et al. 2013). It also highlighted that over the Sahel, this long-term warming displays a well-defined and strong trend in Spring, more complex multi-decadal fluctuations in Summer during the monsoon, and a noisy signal without any obvious trend during the colder and dry winter (as recalled in Fig. 1). These findings were corroborated by several datasets (CRU, local SYNOP data), and well captured by the combined ECMWF ERA40 and ERA-Interim reanalyses[1] (Fig. 1, top panel).

In this complementary report, we first present fundamental features of the diurnal structure of this spring warming. This include its diurnal properties, as inferred from measurements of minimum and maximum daily temperatures and their difference, the diurnal temperature range (DTR), and its departures from the lower troposphere warming.
Using more recent observations provided by AMMA-Catch, we then discuss the annual cycle of temperature and identify the couplings arising between DTR, water vapour and longwave radiation. We conclude with a discussion of the physical processes that potentially accounts for part of the observed multi-decadal trend in the annual cycle of temperature.

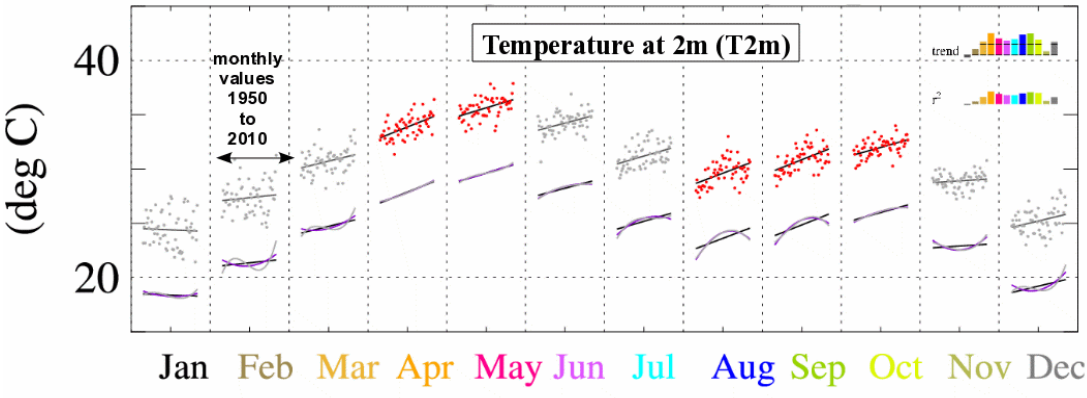

***Figure 1**: Trends in the annual cycle of temperature in the Central Sahel: SYNOP data of Homori from 1950 to 2010. For each months, the series of dots correspond to the series of monthly-mean values obtained for each consecutive year. A linear fit is added, and, for comparison, second and third order fits are displayed just below. The trends over the 60-year period are also indicated for each month on the top-right corner of each plot as well as the values of correlation coefficients (coloured bars).Dots are shown in red when the correlation coefficient is greater than 0.4.*

1 *Note that the shorter duration MERRA and NCEP-CFSR reanalyses on the other hand did not match the observational records over the last three decades. The poor performance of MERRA and NCEP-CFSR compared to ERA-Interim could be related to the assimilation of a smaller amount of data. In addition, such a time period appears as really short to draw inferences about longer term trends as discussed in D1.1.a.*

2. Datasets

As presented in D1.1a, we make extensive use of measurements of temperature at 2m above the surface (T2m) that has been recorded by several tens of meteorological stations over the past decades. These include recorded SYNOP data (those that have been archived by meteorological centres such as the ECMWF), and the Hombori SYNOP dataset provided by Mougin and colleagues. This dataset is representative of the Central Sahel, and has been prepared from more extensive resources including archives from the Meteorology of Mali.

Humidity measurements provided by SYNOP datasets have been explored, but many of them are difficult to exploit in practice because of very numerous holes and erroneous values in time series. This is also obvious over the Sahel when looking at one the rare dedicated gridded product[2] to date, the HadCRUH (Willett et al. 2008). Note also that this dataset actually documents the past 30 years, which is a limitation in terms of analysis of climatic trends. Indeed, Willett et al. (2008) emphasize an overall increase of surface air specific humidity (qv) over land since 1979, while, in sharp contrast, Simmons et al. (2010) point to a substantial drying over land since 1999 (in terms of relative humidity but also qv), and they find it to be especially strong over the Sahel.

With these elements in mind, we make use of the more complete and more quality-checked relative humidity field provided by the Hombori SYNOP dataset which also extends back in time further. (Note that surface pressure was not provided, so in order to estimate specific humidity, simple assumptions have been made for surface pressure, and these should be further refined.)

Regarding water vapour, we also explored the results provided meteorological re-analyses. This includes ERA-40 reanalysis (Uppala et al. 2005), ERA-Interim (Dee et al. 2011), MERRA (Rienecker et al. 2011) and NCEP-CFSR (Saha et al. 2010). Note that for MERRA, we found suspicious long-term fluctuations in qv at 2m that seem to result from precipitation soil-moisture couplings. The wrong depiction of the inter-annual variability of rainfall strongly controls the time series of qv and this prevents further use of this dataset for an analysis of qv multi-decadal trends.

On the other hand, the ECMWF reanalyses ERA-Interim and ERA-40 (which was found to perform overall better than MERRA and NCEP-CFSR) is further used here as a complement to satellite data (MSU monthly-mean tropospheric temperature, Christy et al. 2000) and surface gridded data (CRU TS3.10, Mitchell and Jones 2005, Harris et al. 2013) in order to compare the surface air and lower troposphere decadal trends.

3. Diurnal signature of the multi-decadal warming

Figure 2 shows, with the same rules as in Fig. 1, the fluctuations of daily minimum and maximum temperatures (Tmin and Tmax) and DTR over the past 60 years. It shows that Tmax has increased the most during the late monsoon months (August and September), not in Spring (Fig. 2, top panel). As for the daily mean temperature, fluctuations during these two months appear to be strongly framed by the multi-decadal changes in rainfall (as illustrated by the shape of the second order fit displayed below). Although the Tmax tendency appears to be more linear in Spring, it is much weaker. Indeed, the large trend observed during this period is actually dominated by the increase of Tmin (Fig. 2, middle panel). It is also interesting to notice that the signal is the more pronounced outside of the cool and dry winter months. Thus, the previously discussed spring and autumn trend maxima in T2m (the strongest, Fig. 1) are accounted for predominantly by an increase of Tmin in Spring, while Tmax and Tmix both equally contribute to the late monsoon trend.

2 *Note that humidity estimates are provided by the CRU TS3.1 dataset over the Sahel. However, complementary information, also provided, reveals a real paucity of the humidity data from which the estimates are obtained for this region.*

The distinct annual structure of Tmin and Tmax trends also lead to a large decrease of DTR outside of the monsoon months (Fig. 2, bottom panel), and this decrease is stronger in late winter and spring. The multi-decadal decrease of DTR is an important climatic manifestation of the global warming of the past century. It was already pointed out several years ago (Karl et al. 1991, 1993, Easterling et al. 1997). More recently, Vose et al. (2005) stressed that it was more prominent prior to 1980 than after when both Tmin and Tmax increased in a similar range. Our results for the Sahel point to a strong seasonality of the DTR trend, with weak tendency during the core monsoon, and, in contrast, large changes in late winter and spring that do not appear to have stopped after 1980.

Interpretations of this change in DTR have also been proposed, notably by Dai et al. (1999), who explored the strength of its links with changes in soil moisture, water vapour and clouds. Departing from Dai et al. (1999) findings, here, it seems very unlikely that local soil moisture plays any role prior to the monsoon, as the soil is essentially dry during this period of the year. At the same time, aerosols can be suspected to potentially play a role at least as important of clouds in the Sahel. However, multi-decadal spring trends of both clouds and aerosols still need to be determined.

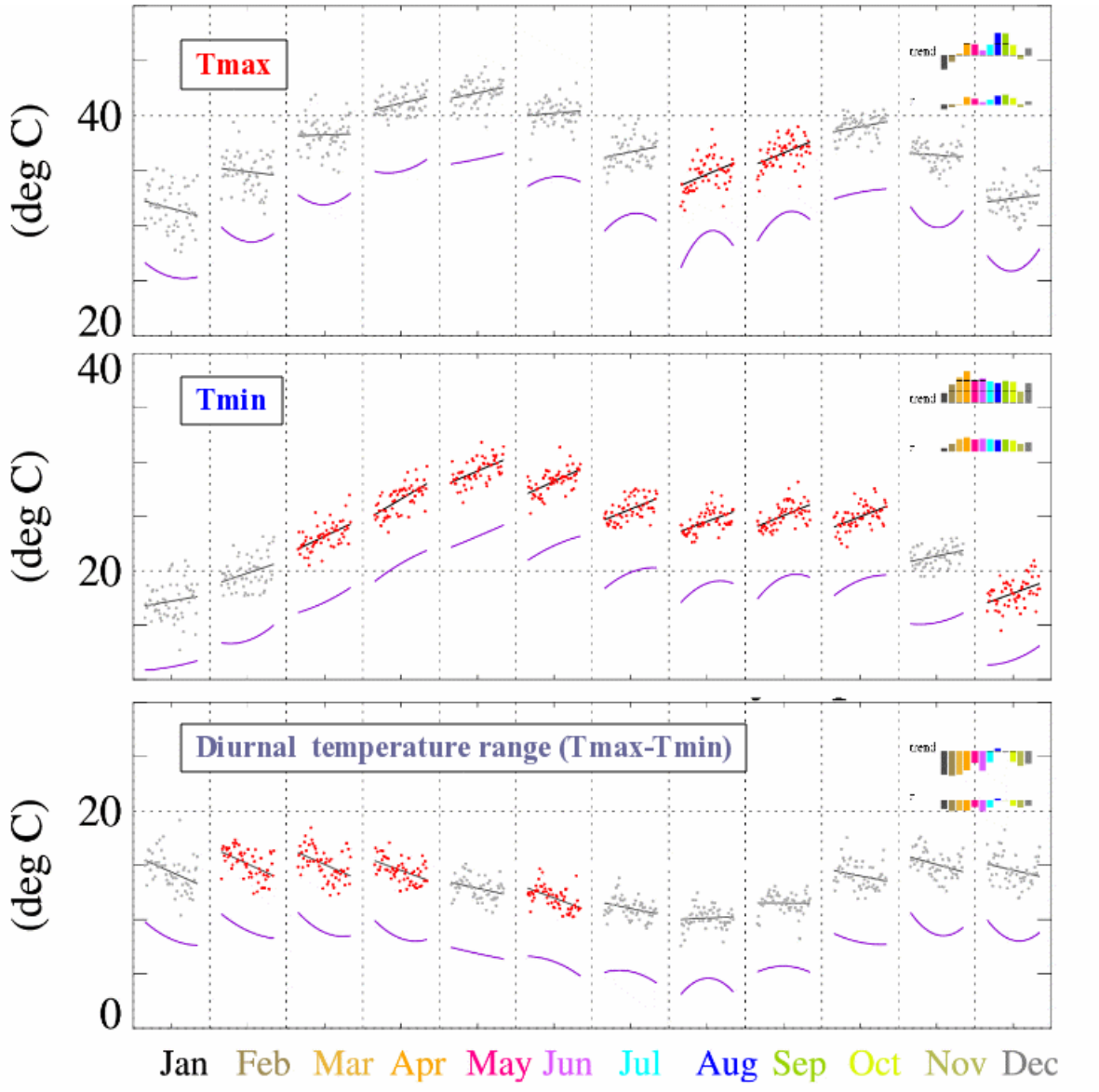

Figure 2*: same as Fig. 1 but for the maximum and minimum daily temperature Tmax (top) and Tmin (middle) and of the diurnal temperature range (DTR=Tmax-Tmin) (bottom).*

4. Diurnal signature of the annual cycle of temperature

Another important piece of information inferred from Fig. 2 is the distinct structures of the annual cycles of Tmin and Tmax in the Sahel. In this figure, it appears that the summer minimum of Tmin is subtantially less pronounced than the one of Tmax. One may also infer that the maximum of Tmin occurs somewhat later (although this is much clearer from analyses of higher-frequency time series). This is better illustrated in Fig. 3, showing annual time series of Tmin and Tmax for the SYNOP station of Ouagadougou, in Southern Sahel, from 1950 to 1980[3]. The transition from winter to spring is also characterized by a much more substantial increase of Tmin compared to Tmax, while the opposite tendency is found from spring, prior to the monsoon, to late summer, during the full monsoon (sharper drop of Tmax compared to Tmin). Figure 3 also emphasizes the annual changes in DTR, with maximum values found in winter, when solar incoming radiation at the top of the atmosphere is the weakest but still substantial while the opacity of the atmosphere (at that time of year very dry) has reached its annual minimum. As a result, daytime temperatures still reach very high values, while the nights remain cool. Note that in Ouagadougou, the maximum temperatures are actually higher in winter than during the monsoon, in summer (this peculiar feature is reversed though when considering higher latitudes in the Sahel).

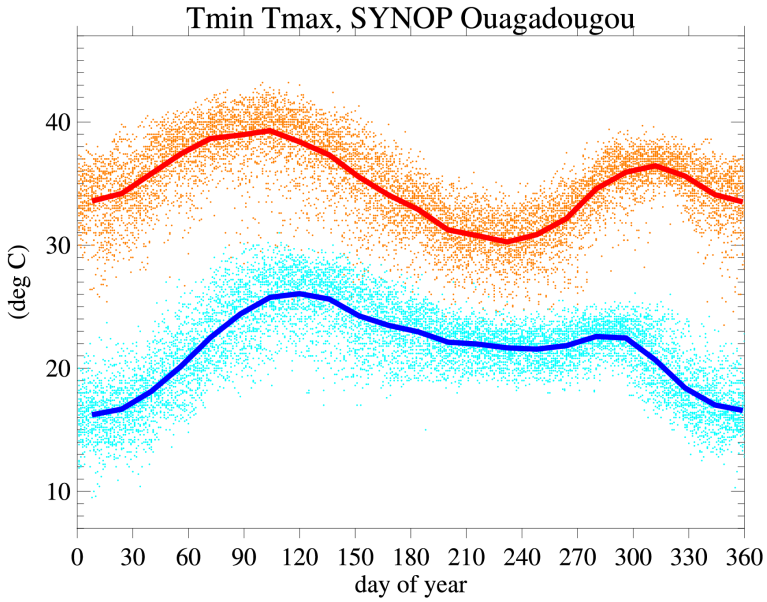

Figure 3*: Time series as a function of day of year of Tmin (blue) and Tmax (orange) at Ouagadougou (SYNOP dataset, covering the period 1950 to 1980). The dots correspond to daily values and the curves to 15-day running mean time average values (using day of year as the time variable).*

The annual dynamic of Tmin and Tmax thus leads to the existence in spring of a period during which Tmax starts to decrease while Tmin still increases as illustrated in Fig. 4. Analysis of daily series indicate that this period can last from a few to several weeks (not shown). They also show that nighttime minimum temperatures increase by several degrees during the first intrusions of the moist monsoon flow arising at that time, possibly linked to the associated increase of the incoming longwave flux. On the other hand, daytime temperature during such moist events often decreases as water vapour, clouds and aerosols then limit the incoming shortwave flux at the surface. Thus, compensating nighttime and daytime processes appear to partly damp the influence of synoptic-scale fluctuations on temperature, but with sharp contrasts in minimum and maximum

3 Note that the values of Tmin and Tmax from SYNOP datasets were not available between about 1980 and the late 90's. Only the values of T2m at specific hours within the day (e.g. 0000 UTC, 0600 UTC, 1200 UTC 1800 UTC) were retrieved by the SEDOO team. As an extension of this work, it would be extremely valuable to retrieve Tmin and Tmax values from the meterorological archives of SYNOP data.

temperature, and in humidity. This also contributes to shape a long lasting yearly maximum of temperature.

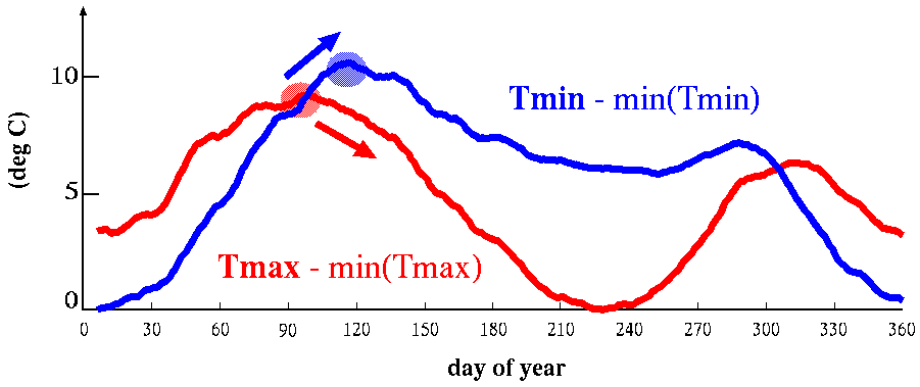

Figure 4*: Annual climatic cycle of Tmin (blue) and Tmax (red) at Ouagadougou. Note that for each curve, the annual mean had been removed. The disk correspond to the annual maximum, and the arrow indicate the sign of the tendency of Tmin and Tmax following the annual maximum of Tmax.*

These findings have been corroborated and quantified by an analysis of several Sahelian SYNOP datasets which is summarized in Fig. 5. We had first considered the several tens of station data available since 1979. Here, only the stations for which sufficient data were available to provide a reasonable climatic depiction of the annual cycles of Tmin and Tmax have been retained (in practice covering more than 25 years). Furthermore, because only SYNOP temperature recorded at specific hours in the day had been made available for the full time period, we used temperature recorded at 0600 UTC and 1200 UTC respectively as proxy for Tmin and Tmax (monthly-mean values of temperature at 1200 UTC in particular are expected to be systematically lower than their counterpart for Tmax). Figure 5 indicates the robustness of the features discussed together with the delicacy of the annual cycle in the Sahel, with a well-defined meridional gradient in the timing and amplitude of the annual maxima and more broadly extrema.

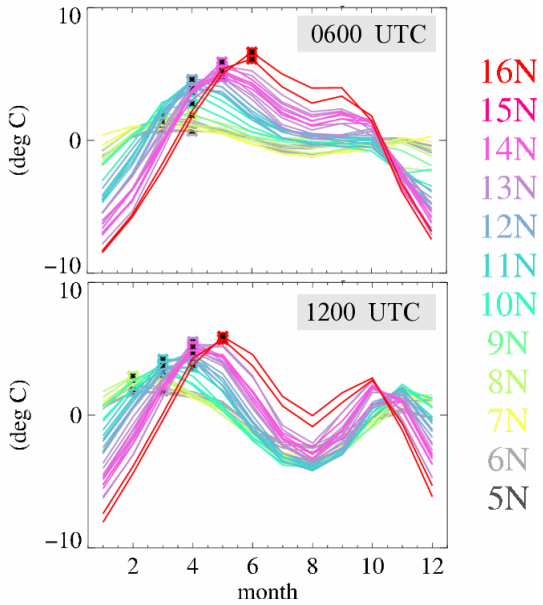

Figure 5*: Annual cycle of T2m at 0600 UTC (upper panel) and 1200 UTC (lower panel) as a function of latitude (color code) in the Sahel (East of 10°W in order to exclude locations where the Atlantic ocean exert a major influence on the annual cycle of temperature) for more than 20 SYNOP stations. Here T2m monthly-mean departures from the yearly-mean values are shown.*

The peculiar balance of nighttime and daytime processes that constrains daily temperature fluctuations in Spring are likely to play a role in the relatively weak short-term (less than 10 years) interannual variability of temperature. Conversely, they may partly account for the very well-defined spring warming in the Sahel, if the later is to be interpreted as a regional manifestation of the larger-scale climatic warming.

5. Comparison of the multi-decadal warming at the surface and in the lower troposphere

In this section, we further analyses the similarities and differences obtained between the warming depicted by surface data and upper air datasets that document a thick lower atmosphere layer. This investigation is motivated by the diurnal subtleties of the annual and multi-decadal fluctuations of surface air temperature that are not expected to affect the tropospheric layer in the same way (namely, the atmosphere typically displays very weak diurnal fluctuations above the boundary layer). Upper air temperature trends can be inferred from a few dedicated satellite datasets but they do not extend prior to the late 70's. This is why the comparison is restricted here to the 1980-2010 period. The tropospheric trend estimated from the MSU dataset is broadly consistent with the surface trend obtained with the CRU TS3.10 dataset (Fig. 6, upper and lower panel), and both results are in broad agreement with the results of Collins (2011). The two estimates both show stronger trends in the Sahel and Sahara than in the Soudanian region. On the other hand, the 'MSU trend' is also consistent with the trend at 700 hPa indicated by ERA-Interim, and again, at the surface, the CRU and ERA-Interim display a reasonable agreement (with substantial differences in the Sahara though, which could be linked to the scarcity of available data there). However, a major difference arise in terms of amplitude with a much stronger amplitude at the surface than higher up in the atmosphere (compare upper and lower panels of Fig. 6). This result points to the limitations of inferences that can be drawn about surface air temperature from satellite data or upper air datasets alone, they also suggest a major importance of processes affecting the lower atmosphere in shaping the observations at the surface and their long-term trends.

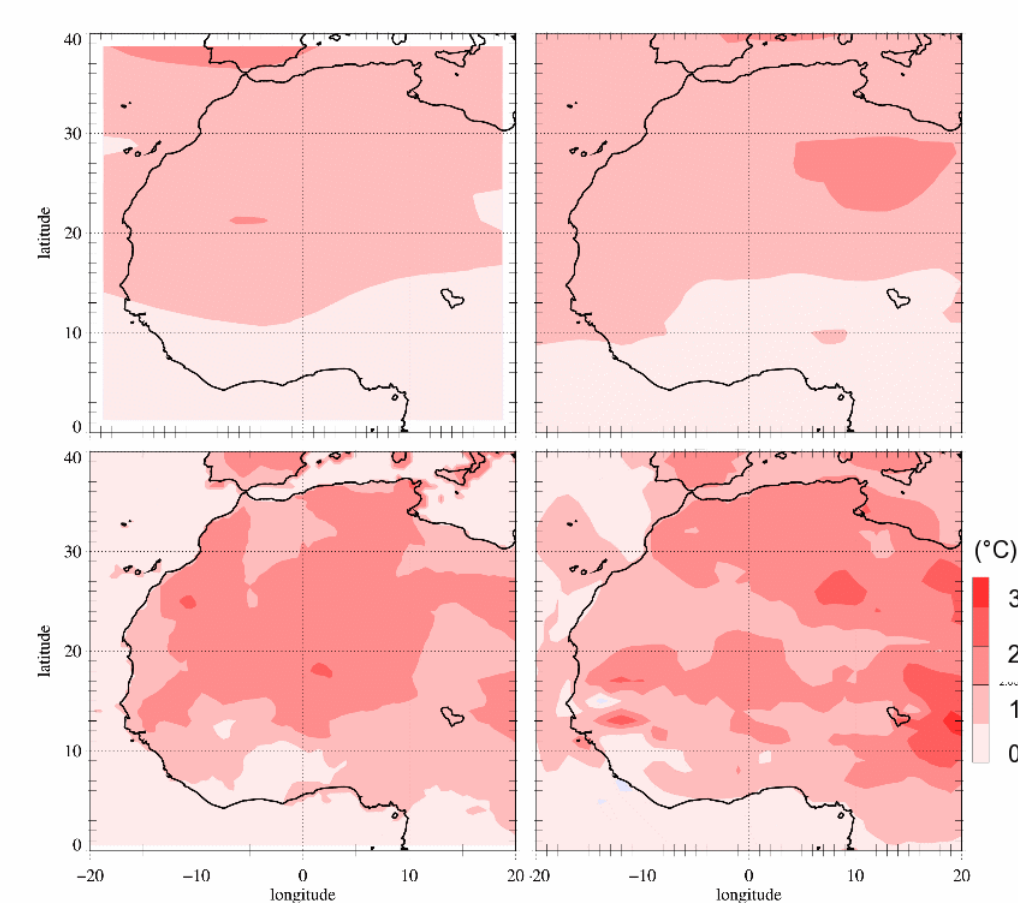

Figure 6*: Trends in temperatures between 1980 and 2010 (showing the result of the month for which this trend is maximum); upper-left panel: for the a thick tropospheric layer (0-8 km, MSU data), upper-right panel: at 700 hPa with ERA-Interim, lower-left panel: at 2m with CRU TR3.10 and lower-right panel at 2m with ERA-Interim.*

6. Thermodynamic-energetic couplings in the amplitude of the diurnal cycle

As can be assessed from previous sections, the diurnal cycle of temperature displays very large changes during an annual cycle, and also throughout the last 60 years. Betts (2006) suggest a major control of surface radiative fluxes on surface air temperature, more precisely a control by the net surface longwave radiation (LWnet), which also quantify the thermal (de)coupling between the soil and the atmosphere. We have tested this idea with the high-frequency AMMA-Catch datasets which are available for the recent year. In short, a normalized temperature diurnal departure is defined, which is inversely proportional to the daily mean LWnet. The results are illustrated in Fig. 7. The upper panel shows how temperature and DTR fluctuates throughout the year, while the middle panel demonstrates the efficiency of the normalization, as manifested by fluctuations of the normalized T2m which are now much less from one month to the next, the main departures being found during the monsoon month, especially in August and September. An analysis of the other AMMA-Catch sites reveal that this finding remains valid as long as the Sahel is considered, i.e. the Soudanian Oueme site (cyan curve in Fig. 7 lower panel) does not obey to the same radiative control.

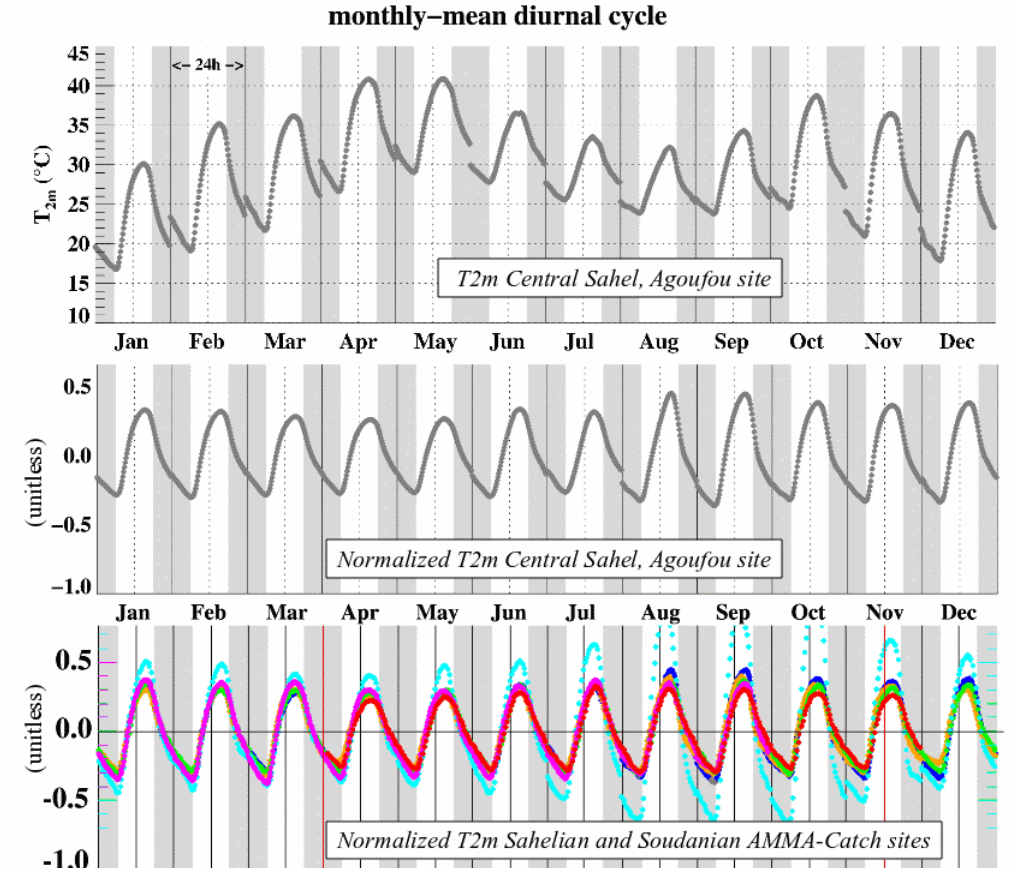

Figure 7*: Monthly-mean diurnal cycles of temperature (upper panel) and normalized temperature (middle panel) in Agoufou, close to Hombori, and for the AMMA-Catch sites (the results for Soudanian Oueme site, located more to the South, are displayed with cyan) .*

On the other hand, LWnet is strongly coupled to relative humidity at the surface, or equivalently, the lifting condensation level that can be estimated from surface relative humidity and pressure (see Betts 1997). This coupling was pointed out by Guichard et al. (2009) for the summer months in the Sahel and has been extended here to the full year. It is found to arises even at the short time scales explored with daily mean values in Fig. 8. In short, when the atmosphere is more humid, LWnet is found to increase. In other words, this result indicates that the DTR provides valuable information on surface humidity and on the couplings between the water and surface

energy cycles, at least for the recent years. Note that we also found strong couplings between precipitable water (estimated by GPS) and the incoming longwave radiative flux (not shown), which translate the increasing opacity of the atmosphere as the atmosphere becomes moister. Overall, these results points to the radiative importance of water vapour outside of the monsoon months, and especially in spring. They also raise the question of a possible role of this process in the observed multi-decadal DTR trend and this is an area that we are currently exploring as briefly discussed and illustrated in the next and final section.

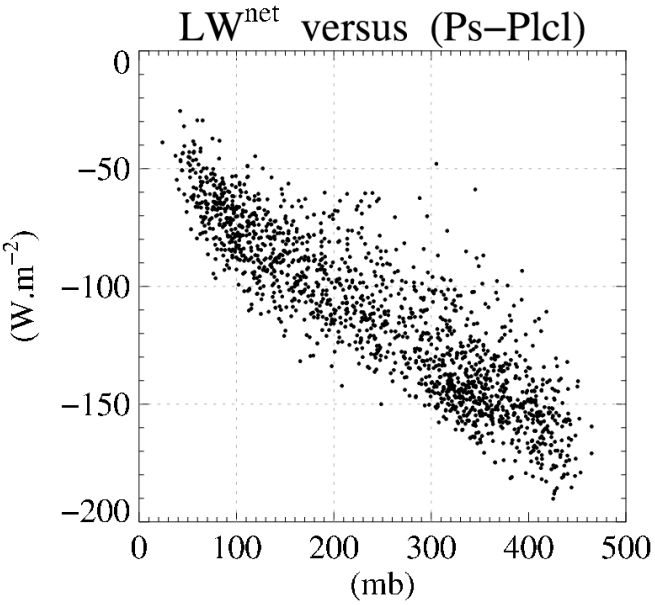

Figure 8*: Scatter diagram of daily-mean LWnet versus lifting condensation level (Agoufou site, result obtained with several years of data).*

5. Conclusion

In this study, we have documented and discussed the diurnal cycle of the strong multi-decadal warming trend observed in the Sahel, mostly with the help of long-term series of minimum and maximum daily temperature (Tmin and Tmax) provided by SYNOP data. For numerous reasons, from both the geophysics and the societal sides, we found it valuable to consider the Sahelian-specific structure of the multi-decal warming within the context of the climatological diurnal and annual cycles of temperature observed in this region.

First, the analysis emphasizes the distinct structures of the annual cycle and of the multi-decadal trends of Tmin and Tmax (Figs 2 to 5), which underlines the importance of processes shaping the diurnal cycle of air temperature at the surface. Indeed, the diurnal temperature range (DTR=Tmax - Tmin) also displays a particular large multi-decadal trend outside of the monsoon season, especially in late winter and spring (Fig. 2). This diurnal signature of warming, with a stronger nighttime than daytime trend, may partly account for the weaker tropospheric warming (Fig. 6).

From an annual cycle perspective, the DTR is found to be largely controlled by the surface net radiation, LWnet (Fig. 7) and LWnet in turn is strongly coupled to the surface air humidity all year long (Fig. 8). We have started to explore the long-term fluctuations in surface humidity and their potential couplings with the warming trend. However, both relative and specific humidity (qv) display complex structures with, for instance, a bimodal distribution daily qv. In addition, the radiative impact of water vapour is not expected to be linearly related to its amount. Keeping these considerations in mind, Hombori SYNOP data suggest the existence of an increase of qv at a multi-

decadal time scale. Furthermore, they point to joint fluctuations of DTR and qv, and qv and T2m in spring, with a spring decrease of DTR coupled to a moistening, the later in turn begin coupled to a warming (Fig. 9). Much work is still to be done in order to assess the robustness of these preliminary findings and to fully understand the underlying processes at play, but they suggest that a local positive water vapour feedback may possibly play an important role in the observed Sahelian long-term spring warming.

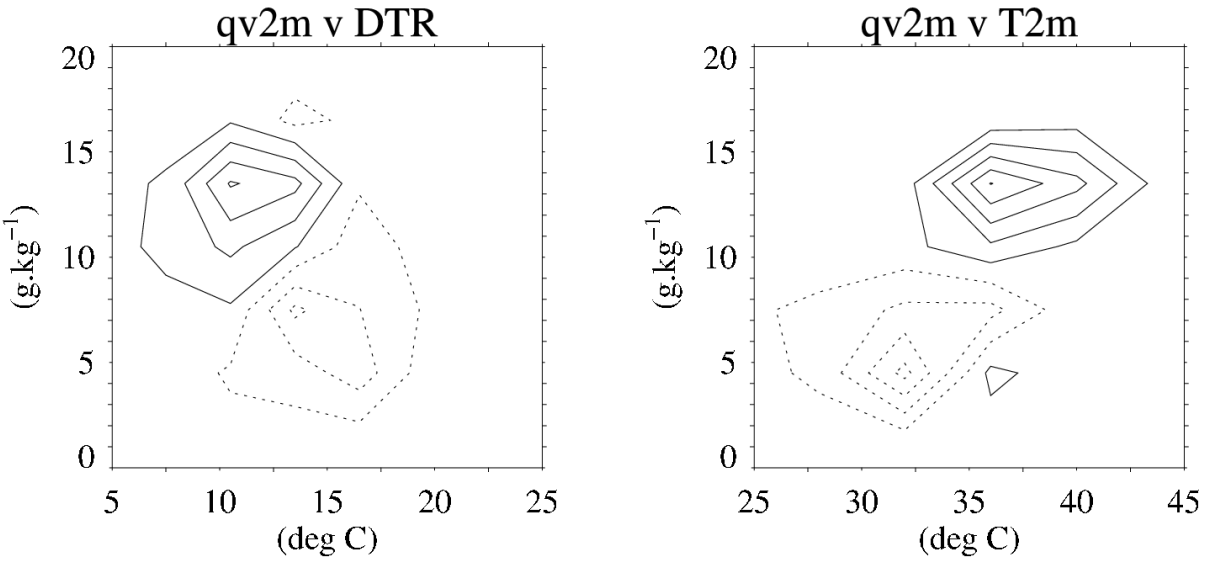

Figure 9*: Differences of the joint probability distributions of DTR and qv2m (left panel) T2m and qv2m (right panel) for April and May in Hombori as obtained over 1990-2010 minus 1950-1970 (SYNOP data), the interval between isolines is 0.02% and the distributions make use of 4°C, 3°C and 3g/kg bins for respectively T2m, DTR and qv .*

6. REFERENCES

Betts, A.K., 1997: Trade Cumulus: Observations and Modeling. Chapter 4 (pp 99-126) in The Physics and Parameterization of Moist Atmospheric Convection, Ed. R. K. Smith, NATO ASI Series C: Vol. 505, Kluwer Academic Publishers, Dordrecht, 498pp.

Betts, A. K., 2006: Radiative scaling of the nocturnal boundary layer and the diurnal temperature range, J. Geophys. Res., 111, D07105, doi:10.1029/2005JD006560.

Christy, J. R., R. W. Spencer, W. D. Braswell, 2000: MSU tropospheric temperatures: dataset construction and radiosonde comparisons. *J. Atmos. Oceanic Technol.*, 17, 1153-1170.

Dai, A., K.E. Trenberth and T.R. Karl, 1999: Effects of clouds, soil moisture, precipitation, and water vapor on diurnal temperature range. J. Climate, 12, 2451–2473. doi: 10.1175/1520-0442(1999) 012<2451:EOCSMP>2.0.CO;2

Dee D. P. and Coauthors 2011: The ERA-Interim reanalysis: configuration and performance of the data assimilation system. Q.J.R. Meteorol. Soc., 137, 553–597. doi: 10.1002/qj.828

Guichard F., L. Kergoat, E. Mougin, F. Timouk, F. Baup, P. Hiernaux and F. Lavenu, 2009: Surface thermodynamics and radiative budget in the Sahelian Gourma: seasonal and diurnal cycles. J. Hydrol., 375, 161-177

Easterling, D.R., Horton, B., Jones, P.D., Peterson, T.C., Karl, T.R., Parker, D.E., Salinger, M.J., Razuvayev, V., Plummer, N., Jamason, P. and Folland, C.K. 1997. Maximum and minimum temperature trends for the globe. Science 277: 364-367.

Harris, I., Jones, P.D., Osborn, T.J. and Lister, D.H., 2013: Updated high-resolution grids of monthly climatic observations – the CRU TS3.10 Dataset. Int. J. Climatol.. doi: 10.1002/joc.3711

Karl, T. R., and Coauthors, 1993: A New Perspective on Recent Global Warming: Asymmetric Trends of Daily

Maximum and Minimum Temperature. Bull. Amer. Meteor. Soc., 74, 1007–1023. doi: http://dx.doi.org/10.1175/1520-0477(1993)074<1007:ANPORG>2.0.CO;2

Karl, T.R., Kukla, G., Razuvayev, V.N., Changery, M.J., Quayle, R.G., Helm Jr., R.R., Easterling, D.R. and Fu, C.B. 1991. Global warming: evidence for asymmetric diurnal temperature change. Geophys. Res. Lett.,18, 2253-2256.

Mitchell T. D. and P. D. Jones, 2005: An improved method of constructing a database of monthly climate observations and associated high-resolution grids. International Journal of Climatology, 25: 693–712. doi: 10.1002/joc.1181

Rienecker, M. M., et al., 2011: MERRA - NASA's Modern-Era Retrospective Analysis for Research and Applications. J. Climate, 24, 3624–3648, doi:10.1175/JCLI-D-11-00015.1.

Simmons, A. J., K. M. Willett, P. D. Jones, P. W. Thorne, and D. P. Dee, 2010: Low-frequency variations in surface atmospheric humidity, temperature, and precipitation: Inferences from reanalyses and monthly gridded observational data sets, J. Geophys. Res., 115, D01110. doi:10.1029/2009JD012442.

Uppala S.M. and Coauthors, 2005: The ERA-40 re-analysis. Q.J.R. Meteorol. Soc., 131, 2961-3012. doi:10.1256/qj.04.176

Vose, R.S., D.R. Easterling, and B. Gleason; 2005: Maximum and minimum temperature trends for the globe: An update through 2004. Geophys. Res. Lett., 32, L23822, doi:10.1029/2005GL024379

Willett, K. M., P. D. Jones, N. P. Gillett and P. W. Thorne, 2008: Recent changes in Surface Humidity: Development of the HadCRUH dataset. J. Climate, 21, 5364–5383. doi: http://dx.doi.org/10.1175/2008JCLI2274.1